J|A|C|S COMMUNICATIONS

Published on Web 01/20/2010

Systematic Cross-Linking Changes within a Self-Assembled Monolayer in a Nanogap Junction: A Tool for Investigating the Intermolecular Electronic Coupling

Yair Paska and Hossam Haick*

The Department of Chemical Engineering and Russell Berrie Nanotechnology Institute, Technion - Israel Institute of Technology, Haifa 32000, Israel

Received December 1, 2009; E-mail: hhossam@technion.ac.il

Using organic molecules as active electronic transport components is to no small degree limited by the lateral electrical conduction between the adjacent molecules, where intermolecular coupling(s) occur.[1,2] Understanding this mode of interaction is critical to eliminate charge loss through defective sites in dense device (e.g., memory[3]) arrays or in self-assembled monolayers exhibiting device functionality.[4]

A general strategy to study the intermolecular coupling within a (self-assembled) monolayer of organic molecules would be the use of a series of different molecules that induce a systematic intermolecular interaction.[5] Nevertheless, reliable and reproducible studies have been hindered by a lack of processes that deliberately control the intermolecular interactions between the adjacent organic molecules while keeping the molecular density, conformation, and/or order identical. With these obstacles in mind, we report here on a strategy that would serve as a reliable tool for investigating the intermolecular coupling within self-assembled monolayers. The strategy is expressed in the form of a *planar* nanogap junction (PNJ) device[6] in conjugation with a self-assembled monolayer having a controllable degree of cross-linking between the adjacent molecules, at identical layer coverages and thicknesses.[7] Electrical measurements can be performed then to determine the PNJ electrical properties at various cross-linking degrees, and the results can be correlated with an intermolecular electronic coupling mechanism within the monolayer.

The PNJ devices studied here were fabricated by standard lithography combined with electrochemical deposition (see Supporting Information, section 1). The fabrication process allowed active monitoring and deliberate control of the electrode separation ($\sim$23 $\pm$ 5 Å). Representative Atomic Force Microscopy (AFM) and Transmission Electron Microscopy (TEM) images of the fabricated PNJ devices are presented in the Supporting Information, Figure 1S. The PNJ devices were cleaned by a wet procedure and functionalized with hexyltrichlorosilane (HTS) molecules having degrees of cross-linking ranging between 0% and 45% (see Supporting Information, section 2 and Figure 2S).[7] The molecular coverage and the monolayer thickness, as measured on electrode-free 2D SiO_2/Si substrates,[7] were identical for all samples.

Figure 1 shows a typical current (I) versus applied voltage (V) measurement of a bare PNJ device and four measurements of the same device after HTS modification and following various degrees of cross-linking. The measurements were carried out at room temperature and under a (99.999% purity) nitrogen atmosphere having <0.1 ppm H_2O. As could be seen in the figure, PNJ devices modified with noncrossed HTS molecules yielded lower currents than bare PNJs. This current became lower and lower upon increasing the degree of cross-linking between the adjacent HTS molecules. For example, the current obtained in bare PNJ, noncrossed HTS/PNJ, and 45%-crossed HTS/PNJ devices at a 0.5 V applied voltage was 27, 3, and 0.5 nA, respectively.[8] To understand these observations, the results were analyzed by the Simmons model[9,10] (see Supporting Information, section 3). Using this model, a linear correlation was found between the degree of cross-linking, the effective rectangular barrier height, ϕ_0, and the zero voltage decay parameter, β_0 (see inset of Figure 2b), in consistency with previous results reported on electrode-free 2D SiO_2/Si surfaces.[7,11] These results immediately raise two questions. First, what is the origin of the lateral conduction within the HTS monolayer? Second, how the cross-linking interaction affects the carrier transfer parallel to the monolayer's surface?

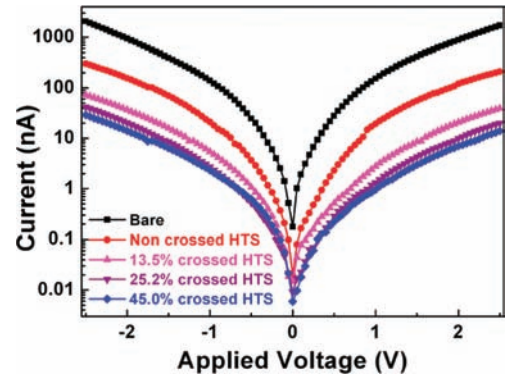

Figure 1. Current (I) as a function of the applied voltage (V) for a bare PNJ device and four devices with different degrees of cross-linking: 0% (noncrossed), 13.5%, 25.2%, and 45%.[8]

A major conduction trajectory in the HTS/PNJ device could be attributed to a direct tunneling (DT) between the adjacent electrodes, above the HTS monolayer (see Figure 2a). The higher current measured in the bare PNJ devices than that predicted by the Simmons model, assuming tunneling decay parameter $\beta \approx 2$ Å^{-1} for free space, excludes this possibility.[8] This finding augments the probability of current decrease due to the electron transfer process at the HTS$-SiO_2$ interface, which, in turn, is determined by the energy of interface states and the electrode's Fermi level.[12] For bridge states having significantly higher energy than the electrode's Fermi level, electron transport occurs by single step superexchange tunneling (ST), i.e. tunneling mediated by interaction between the electrodes and unoccupied states of the organic bridge.[12] In this scenario, the electron transfer rate and, consequently, the junction's current decrease with the junction length, R, according to $I \approx \exp(-\beta R)$. For bridge states comparable in energy with the electrode's Fermi level, electron transport occurs by multiple step sequential hopping (SH); i.e. conduction of an electron occurs through the bridge states, which allow the electron to pass between the electrodes.[12] In this case, the β values are quite low and depend strongly on the molecular structure and applied voltage. To determine which mechanism is more influential, a detailed potential model should be considered.

Obviously, the equilibrium shape of the junction's potential barrier is much more complex than an effective rectangular shape. We propose

10.1021/ja910126s

that the linearity of the effective barrier height is caused by a change in the density of hydroxyl groups[7] within the HTS monolayer, most likely due to the cross-linking process (i.e., the formation of Si−O−Si bonds). Indeed, the formed cross-linking is considered as a sublayer of SiO_2 having energy levels much different than that of the organic layer bridge or electrodes, but it does not change the absolute energy position of the remaining hydroxyl states on the SiO_2 surface. If one accepts this explanation, it is easy to see that the cross-linking changes the number of states in the molecular bridge and, consequently, the average distance between adjacent hydroxyl sites (a_{avr}).

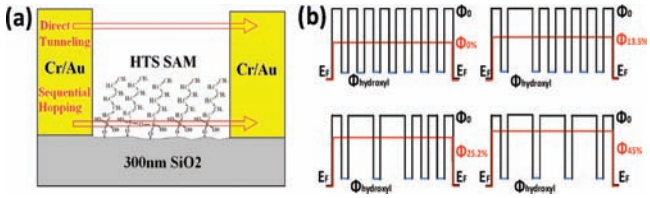

Figure 2. (a) Main potential conduction trajectories in the HTS/PNJ device: direct conduction near and above the SiO_2/HTS interface. (b) Envisioned effective barrier height and potential levels of sequential HTS hydroxyl group.

To extract the potential barriers within the HTS/PNJ device we used the following formula: $\phi_{measured} = (1 - N_i \cdot l/d) \cdot \Delta\phi_{BB} + \phi_{hydroxyl}$ where $\phi_{measured}$ is the measured barrier height, $\phi_{hydroxyl}$ is the hydroxyl's energy state, $\Delta\phi_{BB}$ is the barrier separation between adjacent hydroxyls, d is the junction length (i.e., the distance between the adjacent electrodes), and l is the radius of the hydroxyl group (=0.15 nm); see Figure 2b. Roughly speaking, the junction ($d \approx 23 \pm 5$ Å) can occupy five HTS molecules[13] (one molecule per ~0.21 nm^2 or 1 molecule each ~0.45 nm of the junction's length) and seven hydroxyl states (N_{nc}). The number of the remaining states upon cross-linking can be calculated by $N_i = (1 - \eta)N_{nc}$, where η stands for the cross-linking degree.[7] Under these assumptions, it was found that $\phi_{hydroxyl} = 0.40 \pm 0.01$ eV, $\Delta\phi_{BB} = 2.49 \pm 0.10$ eV, and $\phi_0 = 2.89 \pm 0.10$ eV. An important corollary of these calculations is that the energy level of the hydroxyl states is comparable to the electrode's Fermi level.

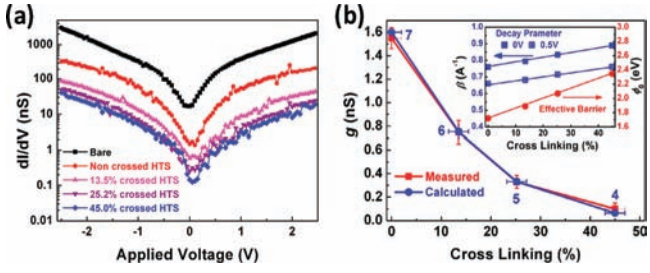

Figure 3. (a) Conduction (dI/dV) as a function of the applied voltage (V) for bare PNJ device and four devices with different degrees of cross-linking. The equilibrium conductions are 17.887 nS for bare PNJ, 1.547 nS for noncrossed-HTS/PNG, 0.788 nS for 13.5% crossed-HTS/PNJ, 0.329 nS for 25.2% crossed-HTS/PNJ, and 0.120 nS for 45% crossed-HTS/PNJ samples. (b) Calculated PNJ conduction, g, as a function of the cross-linking degree. The inset of Figure 3b shows the effective rectangular barrier height, ϕ_0, at 0 V and 0.5 V equilibrium states and the decay parameters, β, as a function of the cross-linking degree.

Putting our results in a wider perspective reveals three main findings: (i) the bare and HTS/PNJ devices exhibit higher current levels than axial junctions modified with saturated hydrocarbon and π-conjugated molecules, whether chemically bonded to the electrodes or not (see ref 14 for more details); (ii) the bare and HTS/PNJ devices do not exhibit a sharp increase in current (see Figure 3a), even when a 6 V bias (not presented) is applied, in contrast to what has been reported for *axial* junctions modified with high (~7 eV) HOMO−LUMO gap molecules;[14] and (iii) the decay parameter, β, depends not only on the applied voltage but also on the degree of cross-linking (Figure 3b). Based on these findings we conclude that the hydroxyl states exist in the electrode's energetic window (viz. the hydroxyl groups have comparable energy to the electrode's Fermi levels) and that the studied PNJ devices are determined by the SH mechanism (see Figure 3b and section 4 of the Supporting Information). The ST mechanism controls the electron transfer rate between the adjacent sites, while the SH is responsible for the long-range electron migration along the molecular bridge.[12] Therefore, the electron transfer rates can be expressed in terms of $k_i = k_i^0 \cdot \exp(-\beta_i a)$, where k_i^0 is the pre-exponent factor.

Using physical considerations and knowledge about the aforementioned HTS/PNJ series, we have calculated the PNJ conduction, g, after HTS modification and following various degrees of cross-linking, as detailed in the Supporting Information, section 5. Plotting the g values of the various HTS/PNJ devices as a function of the degree of cross-linking showed excellent correlation with the measured values (see Figure 3b, mainframe), indicating the robustness of our conclusions.

In summary, PNJ devices[6] in conjugation with controllable Si−O−Si cross-linking (or bonds) can be used as a useful tool for investigating lateral intermolecular electronic coupling between adjacent organic molecules. Systematic variations over the degree of cross-linking in monolayers having different backbone structures and/or functional groups would enable further understanding of the (lateral) intermolecular coupling within self-assembled monolayers.[10] Current−voltage vs back gate voltage measurements (in a transistor-based nanogap device)[4] and/or capacitance−voltage at variable temperatures would have further contributions to this endeavor. Ultimately, this knowledge will be of valuable input for obtaining reliable and reproducible performances over molecule-based devices, including dense memory arrays[3] and Self-Assembled Field Effect Transistors (SAMFETs).[4]

Acknowledgment. We acknowledge the Marie Curie Excellance Grant of the FP6, the US-Israel Binational Science Foundation, and the Russell Berrie Nanotechnology Institute for financial support. H.H. holds the Horev Chair for Leaders in Science and Technology.

Supporting Information Available: Formation of bare PNJ and HTS/PNJ devices; representative AFM and TEM images of the studied PNJ devices; application of Simmon's and sequential hopping models; and calculation of HTS/PNJ conduction. This material is available free of charge via the Internet at http://pubs.acs.org.

References

(1) Lüssem, B.; Müller-Meskamp, L.; Karthäuser, S.; Waser, R.; Homberger, M.; Simon, U. *Langmuir* **2006**, *22*, 3021–3027.
(2) Inoue, A.; Mizutani, W.; Ishida, T.; Tokumoto, H. *Appl. Phys. A: Mater. Sci. Process.* **1998**, *66*, S1241–S1244.
(3) Holten, D.; Bocian, D. F.; Lindsey, J. S. *Acc. Chem. Res.* **2002**, *35*, 57–69.
(4) Mathijssen, S. G. J.; Smits, E. C. P.; van Hal, P. A.; Wondergem, H. J.; Ponomarenko, S. A.; Moser, A.; Resel, R.; Bobbert, P. A.; Kemerink, M.; Janssen, R. A. J.; de Leeuw, D. M. *Nat. Nanotechnol.* **2009**, *4*, 674–680.
(5) Song, H.; Lee, H.; Lee, T. *J. Am. Chem. Soc.* **2007**, *129*, 3806–3807.
(6) Haick, H.; Cahen, D. *Prog. Surf. Sci.* **2008**, *83*, 217–261.
(7) Paska, Y.; Haick, H. *J. Phys. Chem. C* **2009**, *113*, 1993–1997.
(8) Samples that were heated at various temperatures up to 70 °C and, subsequently, cooled down to room temperature (under an inert atmosphere) exhibited similar electrical properties to each other and to unheated samples, thus ruling out the presence/effect of any atmospheric layer.
(9) Vilan, A. *J. Phys. Chem. C* **2007**, *111*, 4431–4444.
(10) Akkerman, H. B.; Naber, R. C. G.; Jongbloed, B.; van Hal, P. A.; Blom, P. W. M.; de Leeuw, D. M.; de Boer, B. *Proc. Natl. Acad. Sci. U.S.A.* **2007**, *104*, 11161–11166.
(11) Paska, Y.; Haick, H. *Appl. Phys. Lett.* **2009**, *95*, 233103/1–233103/3e.
(12) Berlin, Y. A.; Ratner, M. A. *Radiat. Phys. Chem.* **2005**, *74*, 124–131.
(13) Zhang, Q.; Zhang, Q.; Archer, L. A. *J. Phys. Chem. B* **2006**, *110*, 4924.
(14) Salomon, A.; Cahen, D.; Lindsay, S.; Tomfohr, J.; Engelkes, V. B.; Frisbie, C. D. *Adv. Mater.* **2003**, *16*, 1881–1890.

JA910126S